

Critical temperature for quenching of pair correlations

A. Schiller, A. Bjerne, M. Guttormsen, M. Hjorth-Jensen, F. Ingebretsen, E. Melby, S. Messelt, J. Rekestad, S. Siem, and S.W. Ødegård

Department of Physics, University of Oslo, P.O.Box 1048 Blindern, N-0316 Oslo, Norway

The level density at low spin in the $^{161,162}\text{Dy}$ and $^{171,172}\text{Yb}$ nuclei has been extracted from primary γ rays. The nuclear heat capacity is deduced within the framework of the canonical ensemble. The heat capacity exhibits an S-formed shape as a function of temperature, which is interpreted as a fingerprint of the phase transition from a strongly correlated to an uncorrelated phase. The critical temperature for the quenching of pair correlations is found at $T_c = 0.50(4)$ MeV.

PACS number(s): 21.10.Ma, 24.10.Pa, 25.55.Hp, 27.70.+q

The thermodynamical properties of nuclei deviate from infinite systems. While the quenching of pairing in superconductors is well described as a function of temperature, the nucleus represents a finite many body system characterized by large fluctuations in the thermodynamic observables. A long-standing problem in experimental nuclear physics has been to observe the transition from strongly paired states, at around $T = 0$, to unpaired states at higher temperatures.

In nuclear theory, the pairing gap parameter Δ can be studied as function of temperature using the BCS gap equations [1,2]. From this simple model the gap decreases monotonically to zero at a critical temperature of $T_c \sim 0.5 \Delta$. However, if particle number is projected out [3,4], the decrease is significantly delayed. The predicted decrease of pair correlations takes place over several MeV of excitation energy [4]. Recently [5], we reported structures in the level densities in the 1–7 MeV region, which are probably due to the breaking of nucleon pairs and a gradual decrease of pair correlations.

Experimental data on the quenching of pair correlations are important as a test for nuclear theories. Within finite temperature BCS and RPA models, level density and specific heat are calculated for e.g. ^{58}Ni [6]; within the shell model Monte Carlo method (SMMC) [7,8] one is now able to estimate level densities [9] in heavy nuclei [10] up to high excitation energies.

The subject of this Letter is to report on the observation of the gradual transition from strongly paired states to unpaired states in rare earth nuclei at low spin. The canonical heat capacity is used as a thermometer. Since only particles at the Fermi surface contribute to this quantity, it is very sensitive to phase transitions. It has been demonstrated from SMMC calculations in the Fe region [11–13], that breaking of only one nucleon pair increases the heat capacity significantly.

Recently [14,15], we presented a method for extracting level density and γ strength function from measured γ ray spectra. Since the γ decay half lives are long, typically 10^{-12} – 10^{-19} s, the method should essentially give observables from a thermalized system [16]. The spin window is typically 2–8 \hbar and the excitation energy resolution is 0.3 MeV.

The experiments were carried out with 45 MeV ^3He projectiles from the MC-35 cyclotron at the University of Oslo. The experimental data were recorded with the CACTUS multidetector array [17] using the $(^3\text{He}, \alpha\gamma)$ reaction on $^{162,163}\text{Dy}$ and $^{172,173}\text{Yb}$ self-supporting targets. The beam time was two weeks for each target. The charged ejectiles were detected with eight particle telescopes placed at an angle of 45° relative to the beam direction. Each telescope comprises one Si ΔE front and one Si(Li) E end detector with thicknesses of 140 and 3000 μm , respectively. An array of 28 $5'' \times 5''$ NaI(Tl) γ detectors with a total efficiency of $\sim 15\%$ surrounded the target and particle detectors.

From the reaction kinematics the measured α particle energy can be transformed to excitation energy E . Thus, each coincident γ ray can be assigned a γ cascade originating from a specific excitation energy. The data are sorted into a matrix of (E, E_γ) energy pairs. At each excitation energy E the NaI γ ray spectra are unfolded [18], and this matrix is used to extract the primary γ ray matrix, with the well established subtraction technique of Ref. [19].

The resulting matrix $P(E, E_\gamma)$, which describes the primary γ spectra obtained at an initial excitation energy E , is factorized according to the Brink-Axel hypothesis [20,21] by $P(E, E_\gamma) \propto \rho(E - E_\gamma)\sigma(E_\gamma)$. The level density $\rho(E)$ and the γ strength function $\sigma(E_\gamma)$ are determined by a least χ^2 fit to P . Since the fit yields an infinitely large number of equally good solutions, which can be obtained by transforming one arbitrary solution by

$$\tilde{\rho}(E - E_\gamma) = A \exp[\alpha(E - E_\gamma)]\rho(E - E_\gamma), \quad (1)$$

$$\tilde{\sigma}(E_\gamma) = B \exp(\alpha E_\gamma)\sigma(E_\gamma), \quad (2)$$

we have to determine the parameters A , B and α by comparing the ρ and σ functions to known data. The A and α parameters are fitted to reproduce the number of known levels in the vicinity of the ground state [22] and the neutron resonance spacing at the neutron binding energy [23–25].

Figure 1 shows the extracted level densities and γ strength functions for the $^{161,162}\text{Dy}$ and $^{171,172}\text{Yb}$ nuclei. The data for the even nuclei are published recently [5], and are included to be compared to odd nuclei. Also the

γ strength functions are given for all four nuclei. Since other experimental data on the γ strength function in the energy interval 1.5–6 MeV is sparse, we could not fix the parameter B ; and therefore we give the functions in arbitrary units. However, when fitting the functions with the expression $C E_\gamma^n$ we obtain $n \sim 3.9, 4.5$ for the Dy and Yb isotopes respectively, which one would expect from the tale of the giant dipole resonance [14]. In the following, only the level density will be discussed.

The partition function in the canonical ensemble

$$Z(T) = \sum_{n=0}^{\infty} \rho(E_n) e^{-E_n/T} \quad (3)$$

is determined by the measured level density of accessible states $\rho(E_n)$ in the present nuclear reaction. Strictly, the sum should run from zero to infinity. In this work we calculate Z for temperatures up to $T = 1$ MeV. Assuming a Bethe-like level density expression [26], the average excitation energy in the canonical ensemble

$$\langle E(T) \rangle = Z^{-1} \sum_{n=0}^{\infty} E_n \rho(E_n) e^{-E_n/T} \quad (4)$$

gives roughly $\langle E \rangle \sim aT^2$ with a standard deviation of $\sigma_E \sim T\sqrt{2aT}$ where a is the level density parameter. Using Eq. (4) requires that the level density should be known up to $\langle E \rangle + 3\sigma_E$, typically 40 MeV. However, the experimental level densities of Fig. 1 only cover the excitation region up close to the neutron binding energy of about 6 and 8 MeV for odd and even mass nuclei, respectively. For higher energies it is reasonable to assume Fermi gas properties, since single particles are excited into the continuum region with high level density. Therefore, due to lack of experimental data, the level density is extrapolated to higher energies by the shifted Fermi gas model expression [27]

$$\rho_{\text{FG}}(U) = f \frac{\exp(2\sqrt{aU})}{12\sqrt{0.1776} a^{1/2} U^{3/2} A^{1/3}}, \quad (5)$$

where U is the shifted energy and A is the mass number. For shift and level density parameters a , we use von Egidy's parameterization of this expression [28]. The expression had to be normalized by a factor f in order to match the neutron resonance spacing data. The factors are 1.2, 0.94, 0.4 and 0.6 for $^{161,162}\text{Dy}$ and $^{171,172}\text{Yb}$ respectively. The solid lines in Fig. 1 show how the expression extrapolates our experimental level density curves.

The extraction of the microcanonical heat capacity $C_V(E)$ gives large fluctuations which are difficult to interpret [5]. Therefore, the heat capacity $C_V(T)$ is calculated within the canonical ensemble, where T is a fixed input value in the theory, and a more appropriate parameter. The heat capacity is then given by

$$C_V(T) = \frac{\partial \langle E \rangle}{\partial T}, \quad (6)$$

and the averaging made in Eq. (4) gives a smooth temperature dependence of $C_V(T)$. A corresponding $C_V(\langle E \rangle)$ may also be derived in the canonical ensemble.

The deduced heat capacities for the $^{161,162}\text{Dy}$ and $^{171,172}\text{Yb}$ nuclei are shown in Fig. 2. All four nuclei exhibit similarly S-shaped $C_V(T)$ -curves with a local maximum relative to the Fermi gas estimate at $T_c \approx 0.5$ MeV. The S-shaped curve is interpreted as a fingerprint of a phase transition in a finite system from a phase with strong pairing correlations to a phase without such correlations. Due to the strong smoothing introduced by the transformation to the canonical ensemble, we do not expect to see discrete transitions between the various quasi-particle regimes, but only the transition where all pairing correlations are quenched as a whole. In the right panels of Fig. 2, we see that $C_V(\langle E \rangle)$ has an excess in the heat capacity distributed over a broad region of excitation energy and is not giving a clear signal for quenching of pairing correlations at a certain energy [5].

In order to extract a critical temperature for the quenching of pairing correlations from our data, we have to be careful, not to depend too much on the extrapolation of ρ . An inspection of Fig. 1 shows that the level density is roughly composed of two components as proposed by Gilbert and Cameron [27]: (i) a low energetic part; approximately a straight line in the log plot, and (ii) a high energetic part including the theoretical Fermi gas extrapolation; a slower growing function. For illustration, we construct a simple level density formula composed of a constant temperature level density part with τ as temperature parameter, and a Fermi gas expression

$$\rho(E) \propto \begin{cases} \eta \exp(E/\tau) & \text{for } E \leq \varepsilon \\ E^{-3/2} \exp(2\sqrt{aE}) & \text{for } E > \varepsilon \end{cases}, \quad (7)$$

where $\eta = \varepsilon^{-3/2} \exp(2\sqrt{a\varepsilon} - \varepsilon/\tau)$ accounts for continuity at the energy $E = \varepsilon$. If we also require the slopes to be equal at ε , the level density parameter a is restricted to

$$a = \left(\frac{\sqrt{\varepsilon}}{\tau} + \frac{3}{2\sqrt{\varepsilon}} \right)^2. \quad (8)$$

Figure 3 shows the heat capacity evaluated in the canonical ensemble with the level density function of Eq. (7) and $\tau^{-1} = 1.7$ MeV $^{-1}$. The left hand part simulates a pure Fermi gas description, i.e. the case $\varepsilon = 0$, assuming a level density parameter $a = 20$ MeV $^{-1}$. One can see that a pure Fermi gas does not give rise to the characteristic S-shape of the heat capacity as in Fig. 2. The right hand part simulates the experiments, where $\varepsilon = 5$ MeV and a fulfills Eq. (8), i.e. again $a = 20$ MeV $^{-1}$. The characteristic S-shape emerges.

Therefore, our method to find T_c relies on the assumption that the lower energetic part of the level density can be approximately described by a constant temperature level density. Calculating $\langle E(T) \rangle$ and $C_V(T)$ within the canonical ensemble for an exponential level density gives $T^{-1} = \langle E(T) \rangle^{-1} + \tau^{-1}$ and

$$C_V(T) = (1 - T/\tau)^{-2}. \quad (9)$$

Thus, plotting T^{-1} as function of $\langle E(T) \rangle^{-1}$ one can determine τ from Fig. 4. The quantity τ is then identified with the critical temperature T_c , since $C_V(T)$ according to Eq. (9) exhibits a pole at τ and the analogy with the definition of T_λ in the theory of superfluids becomes evident. The $C_V(T)$ curve of Eq. (9) with $T_c = \tau$ using the extracted critical temperatures for the four nuclei is shown as dashed-dotted lines in Fig. 2. This simple analytical expression with only one parameter T_c fits the experimental data up to temperatures of ~ 0.4 MeV. The critical temperature itself is marked by the vertical lines. The extracted T_c is rather close to the estimate of T_c represented by the arrows. The extracted values are $T_c = 0.52, 0.49, 0.50$ and 0.49 MeV for the $^{161,162}\text{Dy}$ and $^{171,172}\text{Yb}$ nuclei respectively, which are somehow delayed compared to a degenerated BCS model with $T_c = 0.5 \Delta$ yielding $T_c \sim 0.48, 0.46, 0.41$ and 0.38 MeV for the respective nuclei, where Δ is calculated from neutron separation energies [22].

We will now discuss how sensitive the extracted critical temperature is with respect to the extrapolation, and we will give an estimate of the uncertainty of the extracted critical temperatures. In the fit in Fig. 4, we use only energies from $\langle E \rangle \sim 0.5\text{--}2$ MeV. This corresponds to energies in the level density curves up to $E_n \sim 6$ MeV according to Eq. (4). Also in Fig. 2, the interval where Eq. (9) fits the experimental data is $T \sim 0\text{--}0.4$ MeV. This corresponds to energies in the level density curves up to $E_n \sim 8$ MeV. Thus, the extracted critical temperature does only depend weakly on the actual extrapolation of ρ curve. Also the S-shape of the $C_V(T)$ curve depends only on the fact, that the nuclear level density develops somehow as a Fermi gas expression at energies somewhere above the neutron binding energy. However, the actual values of the $C_V(T)$ curve above $T \sim 0.5$ MeV do depend on the specific extrapolation chosen.

With respect to T_c , the extrapolation is only important for determining the parameters A and especially α of Eq. (2). We can therefore estimate the error of T_c by

$$\left(\frac{\Delta E \Delta T_c}{T_c^2} \right)^2 = \left(\frac{\Delta a \Delta U}{2\sqrt{a}U_n} \right)^2 + \left(\frac{\Delta D}{D} \right)^2 + 2(0.05)^2, \quad (10)$$

where ΔE is the energy difference between the upper and lower energy where A and α are determined. Δa is the uncertainty of the level density parameter, ΔU is the energy difference between the neutron binding energy and the upper point where A and α are determined, U_n is the (shifted) neutron binding energy. D and ΔD are the neutron resonance spacing and its error. The errors of 5% are added in order to account for the two fitting procedures, one fitting A and α the other fitting T_c , both with an uncertainty of some 5%. Using a very conservative estimate of $a \approx 17.5(6.0)$ MeV $^{-1}$, $U_n < 8$ MeV, $\Delta U < 3$ MeV, $D/\Delta D < 0.2$ and $\Delta E > 4.5$ MeV, we

obtain $\Delta T_c < 0.04$ MeV. This yields a maximum error of T_c of some 8%. It is also important to notice, that due to the strong smoothing in Eq. (4), the errors of the experimental level density curves are negligible in our calculation.

In conclusion, we have seen a fingerprint of a phase transition in a finite system for the quenching of pairing correlations as a whole, given by the S-shape of the canonical heat capacity curves in rare earth nuclei. For the first time the critical temperature T_c at which pair correlations in rare earth nuclei are quenched, has been extracted from experimental data. The reminiscence of the quenching process is distributed over a 6 MeV broad excitation energy region, which is difficult to observe and interpret in the microcanonical ensemble. Simple arguments show that the peak in the heat capacity arises from two components in the level density; a constant temperature like part and a Fermi gas like part. It would be very interesting to compare our results with SMMC calculations performed for a narrow spin window.

The authors are grateful to E.A. Olsen and J. Wikne for providing the excellent experimental conditions. We thank Y. Alhassid for several interesting discussions. We wish to acknowledge the support from the Norwegian Research Council (NFR).

-
- [1] M. Sano and S. Yamasaki, Prog. Theor. Phys. **29**, 397 (1963)
 - [2] A.L. Goodman, Nucl. Phys. **A352**, 45 (1981)
 - [3] A. Faessler *et al.*, Nucl. Phys. **A256**, 106 (1976)
 - [4] T. Døssing *et al.*, Phys. Rev. Lett. **75**, 1276 (1995)
 - [5] E. Melby *et al.*, Phys. Rev. Lett. **83**, 3150 (1999)
 - [6] Nguyen Dinh Dang, Z. Phys. **A335**, 253 (1990)
 - [7] G.H. Lang, C.W. Johnson, S.E. Koonin, and W.E. Ormand, Phys. Rev. **C48**, 1518 (1993)
 - [8] S.E. Koonin, D.J. Dean, and K. Langanke, Phys. Rep. **278**, 1 (1997)
 - [9] W.E. Ormand, Phys. Rev. **C56**, R1678 (1997)
 - [10] J.A. White, S.E. Koonin, and D.J. Dean, Phys. Rev. **C** (to be published)
 - [11] S. Rombouts, K. Heyde, and N. Jachowicz, Phys. Rev. **C58**, 3295 (1998)
 - [12] Y. Alhassid, S. Liu, and H. Nakada, Phys. Rev. Lett. **83**, 4265 (1999)
 - [13] Y. Alhassid, (private communication)
 - [14] L. Henden *et al.*, Nucl. Phys. **A589**, 249 (1995)
 - [15] A. Schiller *et al.*, Nucl. Instrum. Methods (to be published)
 - [16] A. Schiller, M. Guttormsen, E. Melby, J. Rekstad, and S. Siem, Phys. Rev. **C** (to be published)
 - [17] M. Guttormsen *et al.*, Physica Scripta **T32**, 54 (1990)
 - [18] M. Guttormsen *et al.*, Nucl. Instrum. Methods **A374**, 371 (1996)

- [19] M. Guttormsen, T. Ramsøy and J. Rekstad, Nucl. Instrum. Methods **A255**, 518 (1987)
- [20] D.M. Brink, Ph.D. thesis, Oxford University, 1955
- [21] P. Axel, Phys. Rev. **126**, 671 (1962)
- [22] R.B. Firestone and V.S. Shirley, *Table of Isotopes*, 8th edition, (John Wiley & Sons, Inc., New York, Chichester, Brisbane, Toronto, Singapore, 1996), Vol. II
- [23] H.I. Liou, G. Hacken, J. Rainwater, and U.N. Singh, Phys. Rev. **C11**, 462 (1975)
- [24] S.F. Mughabghab and R.E. Chrien, Phys. Rev. **C1**, 1850 (1970)
- [25] H.I. Liou *et al.*, Phys. Rev. **C7**, 823 (1973)
- [26] H.A. Bethe, Phys. Rev. **50**, 332 (1936)
- [27] A. Gilbert and A.G.W. Cameron, Can. J. Phys. **43**, 1446 (1965)
- [28] T. von Egidy, H.H. Schmidt, and A.N. Behkami, Nucl. Phys. **A481**, 189 (1987) Eq. (10)

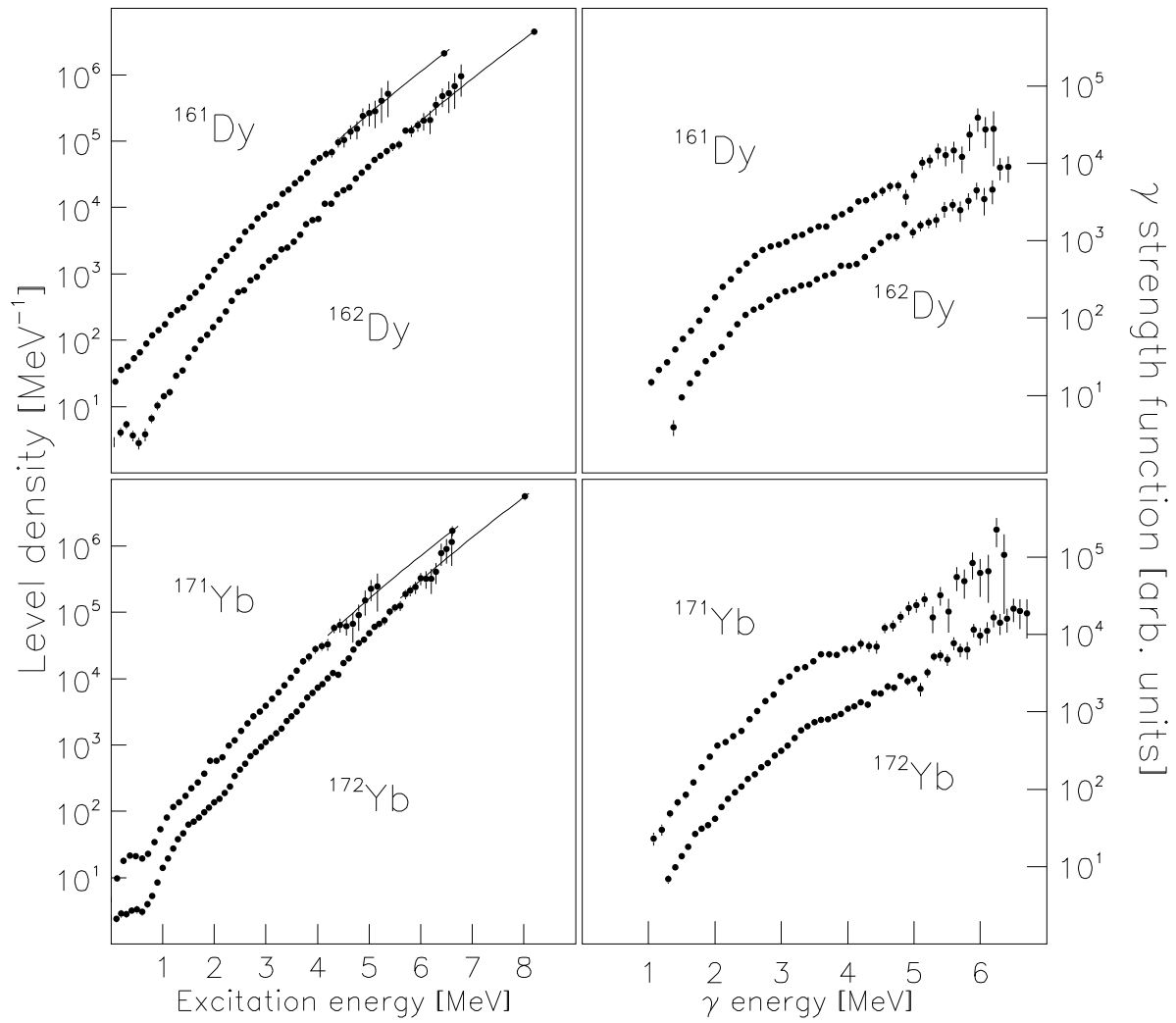


FIG. 1. Experimental level density (points in left panels) and γ strength function (right panels) for $^{161,162}\text{Dy}$ (upper part) and $^{171,172}\text{Yb}$ (lower part). The error bars show the statistical uncertainties. The solid lines are extrapolations based on a shifted Fermi gas model (see text). The isolated point at the neutron binding energy is obtained from neutron resonance spacing data.

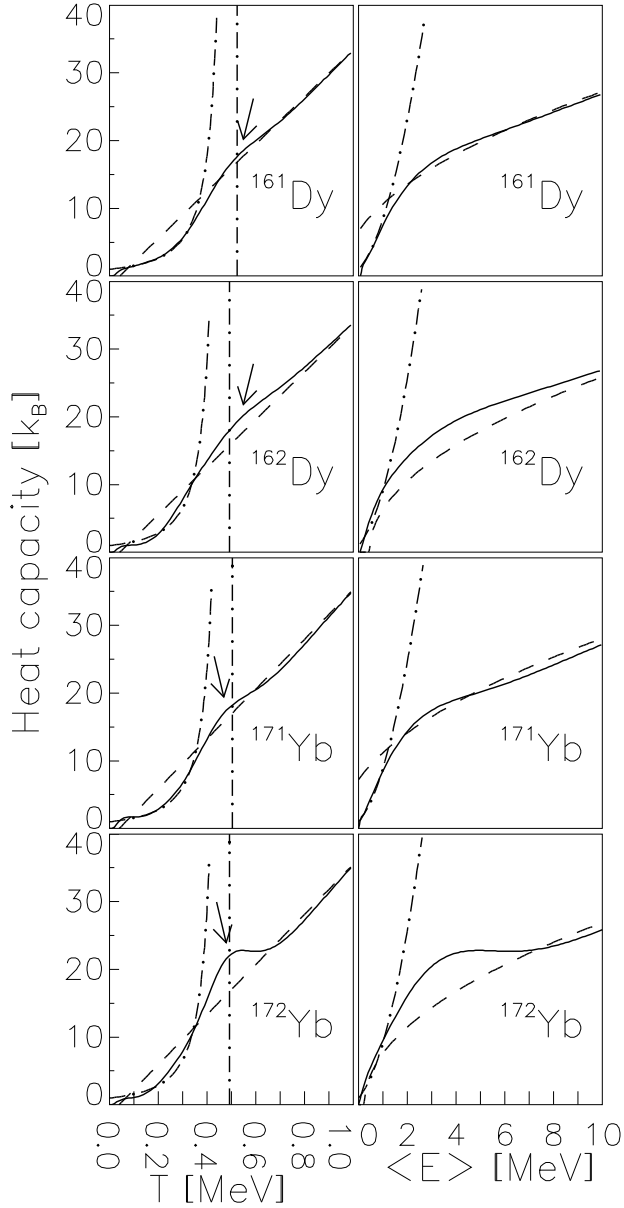


FIG. 2. Semi-experimental heat capacity as function of temperature (left panels) and energy $\langle E \rangle$ (right panels) in the canonical ensemble for $^{161,162}\text{Dy}$ and $^{171,172}\text{Yb}$. The dashed lines describe the approximate Fermi gas heat capacity. The arrows indicate the first local maxima of the experimental curve relative to the Fermi gas estimates. The dashed dotted lines describe estimates according to Eq. (9) where τ is set equal to the critical temperature T_c . T_c is indicated by the vertical lines.

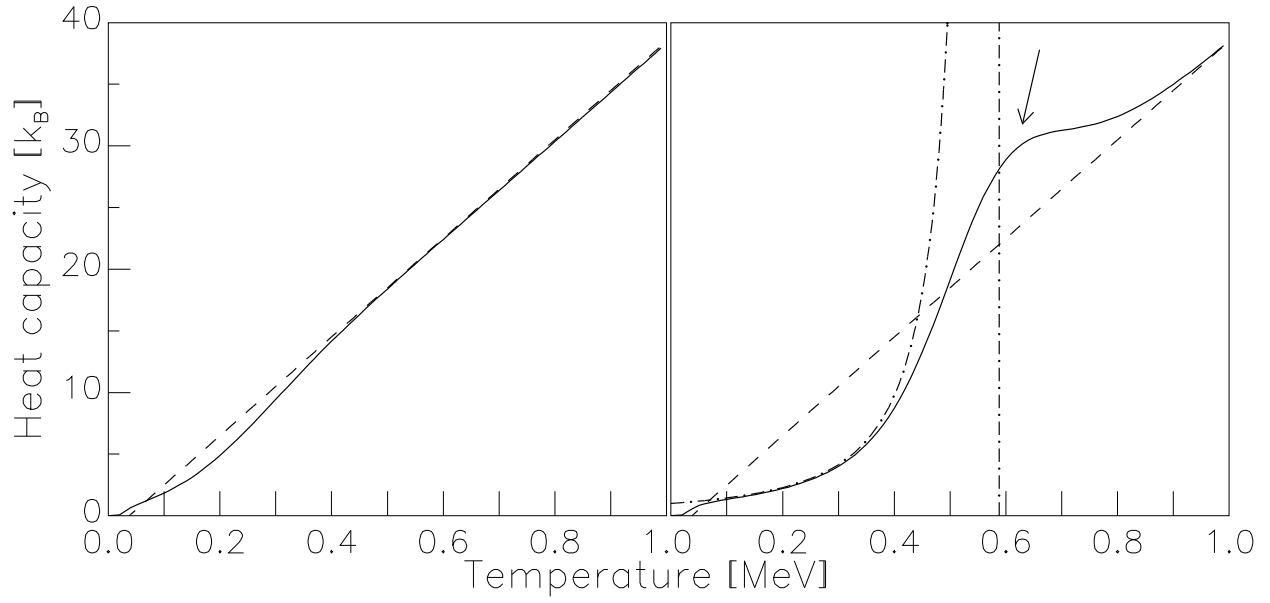


FIG. 3. A pure Fermi gas model cannot give rise to the characteristic S-shape of the canonical heat capacity curve $C_V(T)$ (left panel). A simple composite level density can simulate our experimental findings (right panel).

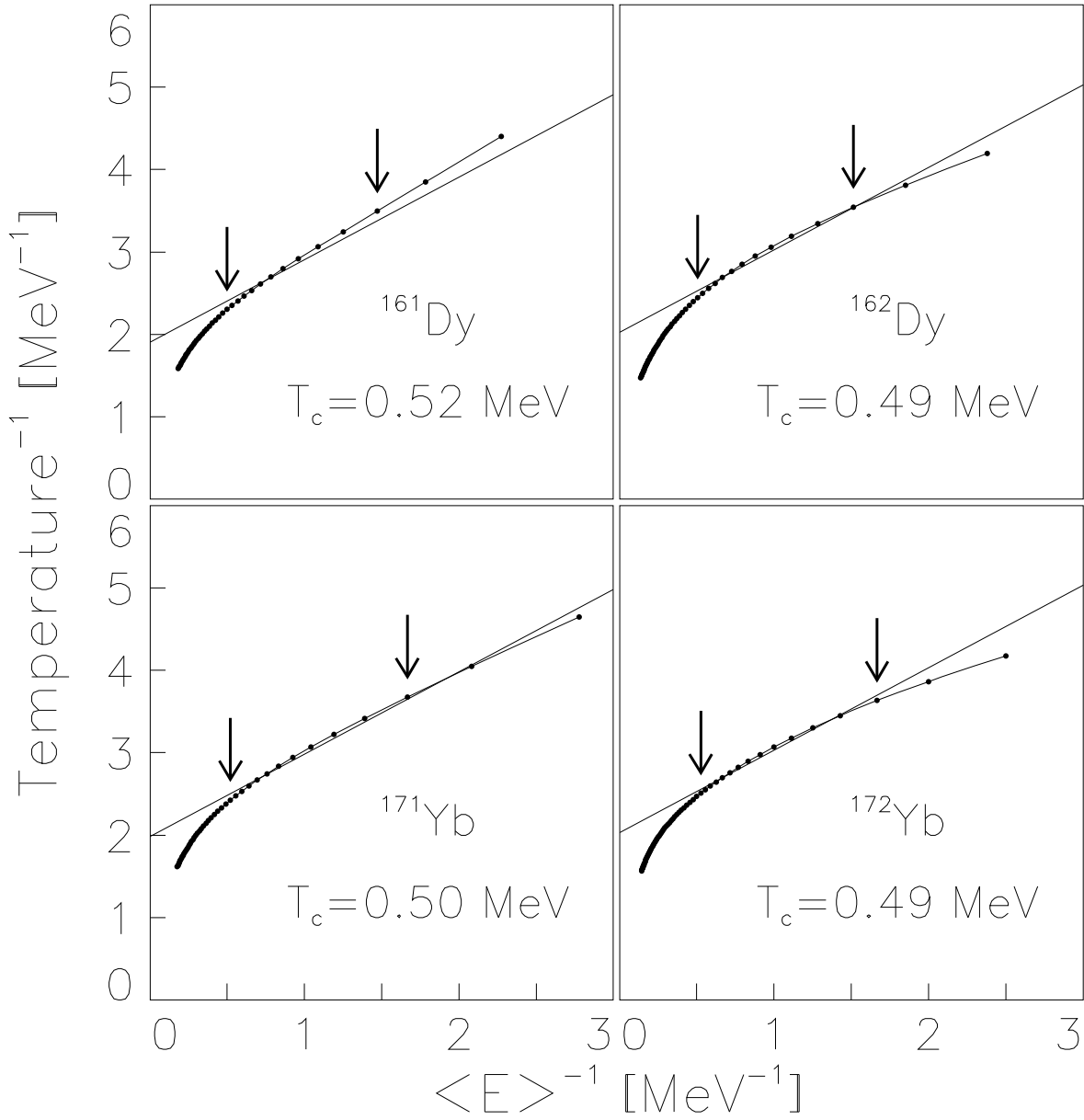


FIG. 4. The critical temperature is deduced by fitting a straight line with slope 1 to the data points between the arrows.